

The extent of Ssa1/Ssa2 Hsp70 chaperone involvement in nuclear protein quality control degradation varies with the substrate

Ramon D. Jones^a, Charisma Enam^a, Rebeca Ibarra^b, Heather R. Borrer^a, Kaitlyn E. Mostoller^a, Eric K. Fredrickson^a, JiaBei Lin^c, Edward Chuang^c, Zachary March^c, James Shorter^c, Tommer Ravid^d, Gary Kleiger^b, and Richard G. Gardner^{a,*}

^aDepartment of Pharmacology, University of Washington, Seattle, WA 98195; ^bDepartment of Chemistry and Biochemistry, University of Nevada, Las Vegas, NV 89154; ^cDepartment of Biochemistry and Biophysics, Perelman School of Medicine, University of Pennsylvania, Philadelphia, PA 19104; ^dDepartment of Biological Chemistry, The Alexander Silberman Institute of Life Sciences, The Hebrew University of Jerusalem, Givat-Ram, Jerusalem 91904, Israel

ABSTRACT Protein misfolding is a recurring phenomenon that cells must manage; otherwise misfolded proteins can aggregate and become toxic should they persist. To counter this burden, cells have evolved protein quality control (PQC) mechanisms that manage misfolded proteins. Two classes of systems that function in PQC are chaperones that aid in protein folding and ubiquitin–protein ligases that ubiquitinate misfolded proteins for proteasomal degradation. How folding and degradative PQC systems interact and coordinate their respective functions is not yet fully understood. Previous studies of PQC degradation pathways in the endoplasmic reticulum and cytosol have led to the prevailing idea that these pathways require the activity of Hsp70 chaperones. Here, we find that involvement of the budding yeast Hsp70 chaperones Ssa1 and Ssa2 in nuclear PQC degradation varies with the substrate. In particular, nuclear PQC degradation mediated by the yeast ubiquitin–protein ligase San1 often involves Ssa1/Ssa2, but San1 substrate recognition and ubiquitination can proceed without these Hsp70 chaperone functions *in vivo* and *in vitro*. Our studies provide new insights into the variability of Hsp70 chaperone involvement with a nuclear PQC degradation pathway.

Monitoring Editor

Orna Cohen-Fix
National Institutes of Health

Received: Feb 12, 2018

Revised: Nov 25, 2019

Accepted: Dec 6, 2019

INTRODUCTION

Most proteins fold into defined structures to accomplish their diverse cellular roles. However, protein folding is dynamic and proteins can misfold into states that alter their function and/or result in aggregation. Protein misfolding is a stochastic process caused by a variety of means including mutations, production errors, improper

nascent peptide folding, and stress-induced damage. The cell manages misfolded proteins by employing protein quality control (PQC) systems that can be broadly categorized into two classes. The protein folding class mitigates the effects of misfolded proteins through the folding, refolding, segregation, and disaggregation activities of protein chaperones (Chen *et al.*, 2011; Verghese *et al.*, 2012). The protein degradation class eliminates misfolded proteins through targeted proteolysis, which in eukaryotes typically involves the ubiquitin–proteasome system (Fredrickson and Gardner, 2012). The combined activities of folding and degradation PQC systems provide the cell with a broad range of capabilities essential to manage the wide variety of misfolded proteins that are generated in the cell.

An open question in the PQC degradation field is how chaperones and ubiquitin–protein ligases cooperate with each other to maintain optimal organellar proteostasis. In many cases, specific chaperones are required for the elimination of misfolded proteins by PQC degradation systems. For example, the mammalian

This article was published online ahead of print in MBoC in Press (<http://www.molbiolcell.org/cgi/doi/10.1091/mbc.E18-02-0121>) on December 11, 2019.

The authors declare no competing financial interests.

*Address correspondence to: Richard Gardner (gardnerr@uw.edu).

Abbreviations used: GAD, Gal4 activation domain; GFP, green fluorescent protein; NLS, nuclear localization signal; PQC, protein quality control; SSA, stress-seventy subfamily A.

© 2020 Jones *et al.* This article is distributed by The American Society for Cell Biology under license from the author(s). Two months after publication it is available to the public under an Attribution–Noncommercial–Share Alike 3.0 Unported Creative Commons License (<http://creativecommons.org/licenses/by-nc-sa/3.0>).

“ASCB®,” “The American Society for Cell Biology®,” and “Molecular Biology of the Cell®” are registered trademarks of The American Society for Cell Biology.

ubiquitin–protein ligase CHIP interacts with Hsp70 chaperones to mediate the ubiquitination and degradation of Hsp70-bound client proteins (Ballinger *et al.*, 1999; Jiang *et al.*, 2001; Murata *et al.*, 2001). In yeast, the endoplasmic reticulum (ER)-membrane ubiquitin–protein ligase Hrd1 requires the Hsp70 chaperone Kar2/BiP to target misfolded proteins in the ER lumen for ubiquitination and degradation (Brodsky *et al.*, 1999; Nishikawa *et al.*, 2001; Taxis *et al.*, 2003; Huyer *et al.*, 2004; Denic *et al.*, 2006). Similarly, the yeast ER-membrane associated ubiquitin–protein ligase Doa10 requires Hsp40 and Hsp70 chaperones for ubiquitination and degradation of misfolded proteins on the cytosolic face of the ER membrane (Huyer *et al.*, 2004; Metzger *et al.*, 2008; Nakatsukasa *et al.*, 2008). Hsp40 and Hsp70 chaperones are also required for ubiquitination and degradation of misfolded proteins targeted by the ubiquitin–protein ligase Ubr1 (Park *et al.*, 2007; Eisele and Wolf, 2008; Heck *et al.*, 2010; Nillegoda *et al.*, 2010; Prasad *et al.*, 2010). From these studies, it is clear that chaperones can play an important role in the degradation process. In most cases, however, the molecular functions of chaperones in PQC degradation have yet to be fully elucidated. One potential role is that chaperones act as substrate-recognition factors and serve as intermediaries between the PQC degradation system and its target substrates. Another potential role for chaperone function in PQC degradation is that they maintain substrate solubility and accessibility. These possibilities are not mutually exclusive and chaperones could serve either or both roles on subsets of misfolded proteins.

Our studies have focused on understanding how misfolded proteins are targeted for PQC degradation in the nucleus. We previously found that the yeast nuclear-localized, ubiquitin–protein ligase San1 functions in the destruction of misfolded nuclear proteins by mediating their ubiquitination for proteasomal degradation (Gardner *et al.*, 2005). We also found that *in vitro* and in bacteria San1 can ubiquitinate misfolded proteins without the aid of chaperones (Rosenbaum *et al.*, 2011; Ibarra *et al.*, 2016), indicating that chaperones are not essential for the recognition of misfolded proteins by San1. However, other studies have shown that the Hsp70 chaperones Ssa1 and Ssa2 are required *in vivo* for San1-mediated ubiquitination and degradation of misfolded proteins that were presumed to be cytosolic but ultimately enter the nucleus (Heck *et al.*, 2010; Prasad *et al.*, 2010, 2012; Brower *et al.*, 2013; Guerriero *et al.*, 2013; Prasad *et al.*, 2018). On the basis of the discrepancies between our studies and those of others, we explored whether there is a universal requirement for the Hsp70 chaperones Ssa1 and Ssa2 in San1-mediated nuclear PQC degradation by using a diverse collection of San1 substrates.

RESULTS

Involvement of Ssa1/Ssa2 in San1-mediated degradation is maintained after active nuclear localization of “cytosolic” substrates

Ssa1/Ssa2 were shown to be required for the degradation of San1 substrates that were initially thought to be in the cytosol (Heck *et al.*, 2010; Prasad *et al.*, 2010, 2012). However, analysis of the substrates' localization revealed that they were enriched in the nucleus (Heck *et al.*, 2010; Prasad *et al.*, 2010, 2012) despite the fact that they are not normally nuclear proteins and lack canonical nuclear localization sequences (NLSs). It is currently unknown how these misfolded proteins enter the nucleus. The sizes of substrates in those studies are below the ~110 kDa passive diffusion limit of the nuclear pore (Wang and Brattain, 2007), suggesting that entry into the nucleus may be through passive diffusion. It is therefore possible that substrates lacking an NLS require Ssa1/Ssa2 for

San1-mediated degradation because these chaperones assist in passive nuclear import. To test this, we examined whether Ssa1/Ssa2 were still required for the degradation of these substrates after active nuclear transport.

To import substrates into the nucleus, we added GFP containing an NLS to three of the previously described “cytosolic” substrates: $\Delta 2\text{GFP}$ (Prasad *et al.*, 2010, 2012), ΔssPrA (Prasad *et al.*, 2010, 2012), and the Von Hippel–Lindau syndrome protein VHL (Samant *et al.*, 2018). After examining the degradation of these NLS^{plus} misfolded proteins in parent, *ssa1* Δ *ssa2* Δ , and *san1* Δ cells, we found that Ssa1/Ssa2 were required for their optimal degradation (Figure 1, A and C). It therefore appears that the Ssa1/Ssa2 dependency in San1-mediated degradation is independent of the nuclear entry mode. In fact, fluorescence microscopy of GFP^{NLS}-VHL revealed that it is predominantly localized to the nucleus in *ssa1* Δ *ssa2* Δ cells, similar to that observed in both parent and *san1* Δ cells (Figure 2A and Supplemental Figure 1A). These results support the idea that the stabilization of San1 substrates in *ssa1* Δ *ssa2* Δ cells is not related to their nuclear transport mechanism.

The extent of Ssa1/Ssa2 involvement in San1-mediated degradation *in vivo* varies with the substrate

On the basis of our findings that GFP^{NLS}- $\Delta 2\text{GFP}$, GFP^{NLS}- ΔssPrA , and GFP^{NLS}-VHL require Ssa1/Ssa2 for optimal degradation, we wanted to determine whether this is a universal feature of San1-mediated degradation. To assess more broadly the Ssa1/Ssa2 involvement in San1-substrate degradation, we examined multiple representative examples from the 40+ San1 substrates that we previously characterized (Gardner *et al.*, 2005; Fredrickson *et al.*, 2011; Rosenbaum *et al.*, 2011). The original class of San1 substrates we identified are those with single missense mutations that cause temperature-dependent misfolding (Gardner *et al.*, 2005; Fredrickson *et al.*, 2011). The second class of San1 substrates we identified is proteins carrying truncations that eliminate portions of the protein most likely required for proper folding (Rosenbaum *et al.*, 2011). The final class of San1 substrates we identified is small hydrophobic peptides that we propose mimic the type of exposed hydrophobicity San1 recognizes in misfolded proteins (Fredrickson *et al.*, 2011, 2013b). We chose five representative substrates from these classes:

1. Two missense mutant substrates that included GAD-Cdc68-1, which is the isolated N-terminal domain of Cdc68 (residues 2–468) containing a G132D mutation (Evans *et al.*, 1998), and GAD-Cdc13-1, which is the isolated N-terminal domain of Cdc13 (residues 1–600) carrying a P371S mutation (Nugent *et al.*, 1996). The same constructs without the missense mutations are not recognized by San1 (Rosenbaum *et al.*, 2011).
2. Two truncated substrates that included GFP^{NLS}-Tef2*, which contains residues 190–458 of the translation elongation factor Tef2 fused to GFP^{NLS}, and GFP^{NLS}-Bgl2*, which contains residues 20–313 of the endo- β -1,3-glucanase Bgl2 fused to GFP^{NLS} (Fredrickson *et al.*, 2011; Gallagher *et al.*, 2014). The full-length constructs are not recognized by San1 (Rosenbaum *et al.*, 2011).
3. One hydrophobic peptide substrate, which was GFP^{NLS}-peptide 6 (RDILVYTYILVYVI fused to GFP^{NLS}; Fredrickson *et al.*, 2011).

Using these substrates, we observed a differential involvement of Ssa1/Ssa2 in San1-mediated degradation (Figure 1, B and C). There was some stabilization for GFP^{NLS}-Tef2*, GFP^{NLS}-Bgl2*, and GFP^{NLS}-peptide 6 in *ssa1* Δ *ssa2* Δ cells (Figure 1, B and C). By contrast, GAD-Cdc13-1 and GAD-Cdc68-1 showed little to no stabilization in

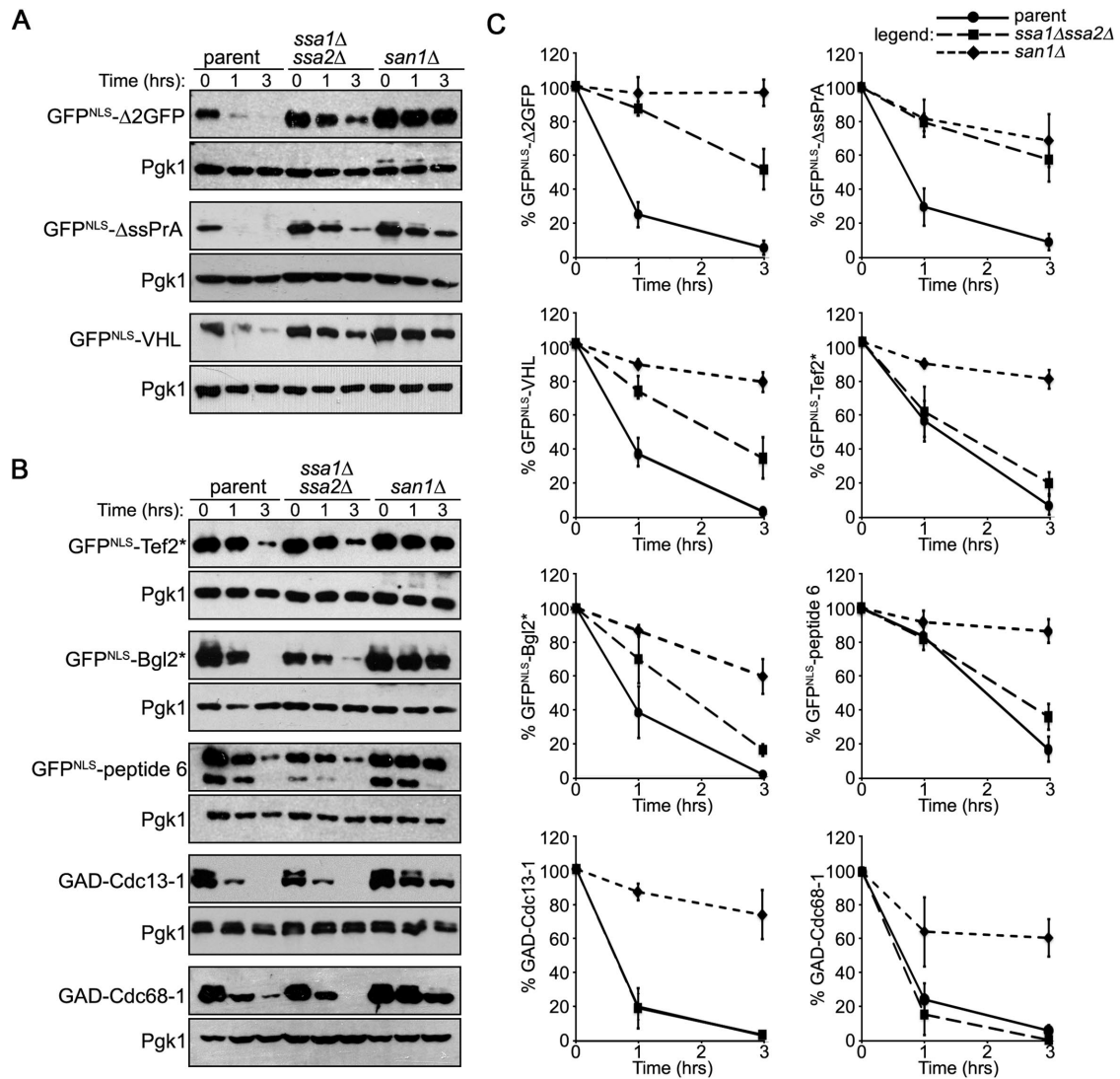


FIGURE 1: The Hsp70 chaperones Ssa1/Ssa2 are not universally required for San1-mediated degradation. (A) Cycloheximide-chase degradation assays were performed on parent, *ssa1Δ/ssa2Δ*, and *san1Δ* cells to assess the stability of GFP^{NLS}- Δ 2GFP, GFP^{NLS}- Δ ssPrA, or GFP^{NLS}-VHL. Time after cycloheximide addition is indicated above each lane. Anti-GFP antibodies were used to detect each substrate. Anti-Pgk1 antibodies were used to assess loading. (B) Cycloheximide-chase degradation assays were performed on parent, *ssa1Δ/ssa2Δ*, and *san1Δ* cells to assess the stability of GFP^{NLS}-Tef2*, GFP^{NLS}-Bgl2*, GFP^{NLS}-peptide 6, GAD-Cdc13-1 or GAD-Cdc68-1 as in A. Anti-GFP and anti-GAD antibodies were used to detect each respective substrate. Anti-Pgk1 antibodies were used to assess loading. (C) Decay curves for the degradation assays in A and B. Band intensities were measured using ImageJ with the levels in the 0 time points for each replicate arbitrarily set to 100%. Standard deviation in each graph was determined from four independent assays conducted for each substrate in each strain.

ssa1Δssa2Δ cells (Figure 1, B and C). The degradation of all substrates tested was dependent on San1 (Figure 1, B and C). By fluorescence microscopy, GFP^{NLS}-Tef2* and GFP^{NLS}-Bgl2*, both of which were partially stabilized in *ssa1Δssa2Δ* cells, did not show observable alterations in their nuclear localization (Figure 2, B and C, and Supplemental Figure 1, B and C), indicating that the stabilization by loss of Ssa1/Ssa2 function is not due to their mislocalization to the cytosol.

The extent of Ssa1/Ssa2 involvement in San1-mediated ubiquitination in vivo also varies with the substrate

From the diversity of Ssa1/Ssa2 involvement in San1-substrate degradation (Figure 1), we examined Ssa1/Ssa2 involvement in San1-substrate ubiquitination. We performed in vivo ubiquitina-

tion assays using GFP^{NLS}-VHL (a strongly Ssa1/Ssa2-dependent San1 substrate), GFP^{NLS}-Tef2* (a weakly Ssa1/Ssa2-dependent San1 substrate), and GAD-Cdc68-1 (a Ssa1/Ssa2-independent San1 substrate) in parent, *ssa1Δssa2Δ*, and *san1Δ* cells (Figure 3). GFP^{NLS}-VHL ubiquitination was reduced in *ssa1Δssa2Δ* cells and the decrease was similar to that observed in *san1Δ* cells (Figure 3A). GFP^{NLS}-Tef2* ubiquitination was reduced in *ssa1Δssa2Δ* cells, but the decreased levels were intermediate between that observed with parent and *san1Δ* cells (Figure 3B). GAD-Cdc68-1 ubiquitination in *ssa1Δssa2Δ* cells was indistinguishable to that observed in parent cells, but strongly reduced in *san1Δ* cells (Figure 3C). Thus, there is a good correlation in the Ssa1/Ssa2 dependency between the ubiquitination and degradation of San1 substrates.

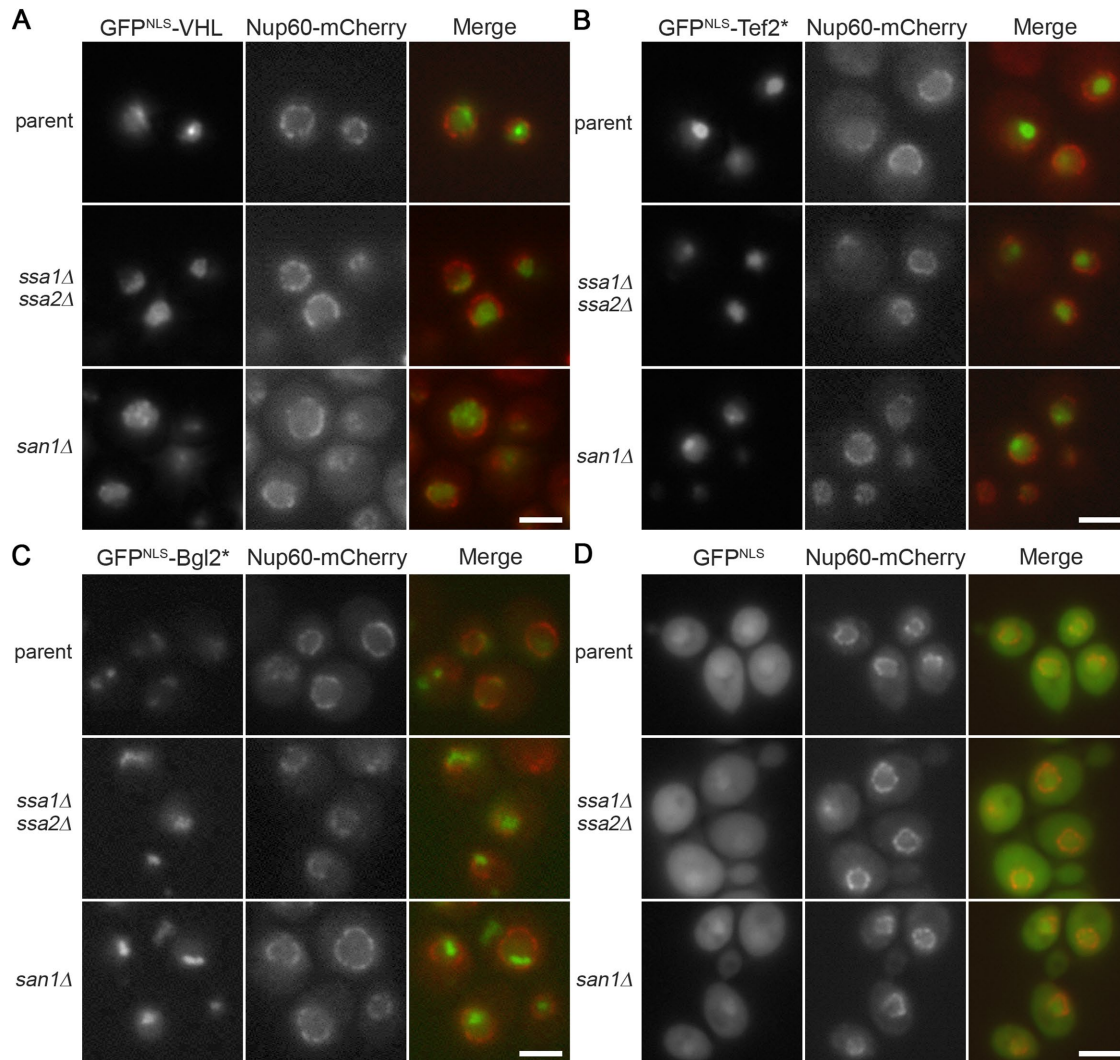


FIGURE 2: Nuclear localization of San1 substrates is unaffected by deletion of *SSA1* and *SSA2*. Cellular localization of GFP^{NLS}-VHL (A), GFP^{NLS}-Tef2* (B), GFP^{NLS}-Bgl2* (C), and GFP^{NLS} as a stable control (D) in parent, *ssa1Δ/ssa2Δ*, and *san1Δ* cells also expressing Nup60-mCherry as a nuclear membrane marker was examined by fluorescence microscopy. Representative cells are shown. Bar equals 2 μm. Microscopy was performed three independent times. Fields containing more cells are shown in Supplemental Figure 1.

Chaperones are dispensable for San1-substrate ubiquitination in vitro

To test chaperone involvement further, we reconstituted San1 substrate ubiquitination in vitro with and without chaperones. Because San1 substrates are constitutively misfolded proteins, we have been repeatedly unable to purify San1's yeast substrates from *Escherichia coli* as they readily aggregate during expression and purification. Indeed, the inability to purify recombinantly produced misfolded proteins is one of the major challenges in reconstituting PQC substrate ubiquitination in vitro, and was the key issue that spurred us to develop a reconstituted San1-ubiquitination assay in bacteria (Rosenbaum *et al.*, 2011). We overcame this hurdle by developing in vitro assays wherein San1 ubiquitinates a conditionally denatured luciferase (Rosenbaum *et al.*, 2011), or a short soluble hydrophobic peptide (Ibarra *et al.*, 2016). Using these in vitro substrates, we hypothesized that chaperone addition would enhance San1-mediated ubiquitination if chaperones were essential for San1-mediated ubiquitination.

The previously described luciferase denaturation and ubiquitination assay (Rosenbaum *et al.*, 2011) was further optimized for these studies. We first determined the optimal temperature for luciferase denaturation that led to robust San1-mediated ubiquitination. We confirmed that 42°C led to the best temporal visualization ubiquitination of luciferase (Figure 4A). Next, we found that San1 readily ubiquitinated denatured luciferase with only the aid of the San1 ubiquitination cascade components (Figure 4C, lanes 5 and 6), but not native luciferase (Figure 4C, lanes 3 and 4). Approximately 30% of denatured luciferase was ubiquitinated by an equimolar amount of San1 within 5 min and 40–45% ubiquitinated by 15 min (Figure 4D).

We then determined the optimal concentration of Ssa1 to use in the in vitro assay by evaluating the amount of Ssa1-Ydj1 that renatures luciferase in the absence/presence of Hsp104 (Glover and Lindquist, 1998; Jackrel *et al.*, 2014). In our assays, 1 μM Ssa1-Ydj1 demonstrated the most robust refolding activity, as measured by the percentage of reactivated luciferase compared with an equivalent

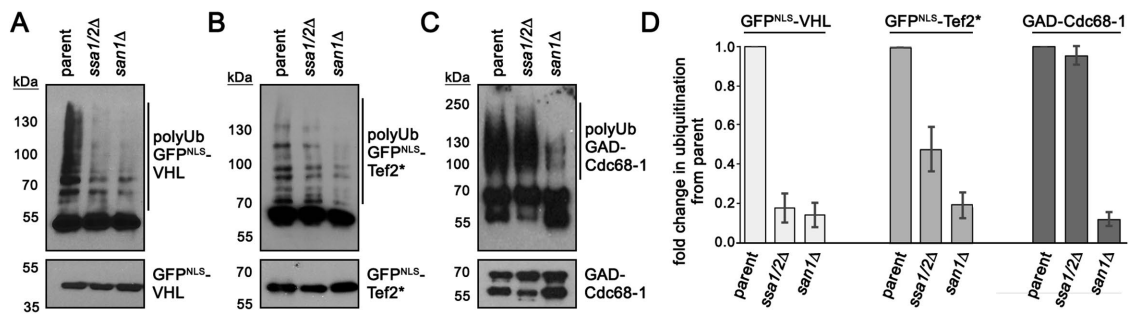


FIGURE 3: Loss of Ssa1/Ssa2 function for San1-mediated substrate degradation similarly affects San1-mediated substrate ubiquitination. In vivo ubiquitination assays were performed to assess the ubiquitination levels of GFP^{NLS}-VHL (A), GFP^{NLS}-Tef2* (B), and GAD-Cdc6-1 (C) in parent, *ssa1Δssa2Δ*, and *san1Δ* cells. Cells were grown to midexponential phase, expression of each substrate was induced by addition of galactose, and cells were lysed. Ubiquitinated proteins were affinity purified using ubiquitin-affinity TUBE agarose beads. Anti-GFP or anti-GAD antibodies were used to detect each respective substrate. Bottom panels represent the amount of each substrate in total lysates. Top panels represent the amount of substrate in the purified ubiquitinated protein pool. (D) Intensities of ubiquitination levels in A–C were measured using ImageJ. Ubiquitination levels in the top panels were normalized against input in the bottom panels. Ubiquitination levels in the parent strains were set to the arbitrary value of 1. Standard deviation in each histogram was determined from three independent assays conducted for each substrate in each strain.

amount of undenatured, native luciferase (Figure 4B). After adding Ssa1 to the in vitro ubiquitination reaction, we observed no enhancement of San1-mediated ubiquitination (Figure 4C, lanes 7 and 8). It has been found that additional chaperones (Hsp104, Ydj1, and Sse1) are required to facilitate refolding of denatured luciferase in vitro (Figure 4B; Glover and Lindquist, 1998; Jackrel *et al.*, 2014). Therefore, we added these chaperones sequentially to the in vitro assay. In no case did the addition of additional chaperones enhance San1-mediated ubiquitination of denatured luciferase (Figure 4C, lanes 9–14).

To explore further whether chaperones assist San1-mediated ubiquitination, we next used the peptide-based in vitro ubiquitination assay (Ibarra *et al.*, 2016). A key advantage of the peptide-based assay is that, while denatured luciferase likely adopts multiple conformations resulting in a heterogeneous population, the peptide is too short for protein folding and is likely more homogeneous than misfolded luciferase. Similar to San1-mediated ubiquitination of luciferase, we found that San1 readily ubiquitinated the peptide substrate with only the aid of the San1 ubiquitination cascade components (Figure 4E, lanes 3 and 4). Intriguingly, the addition of Ssa1 to this assay inhibited the ability of San1 to ubiquitinate the peptide substrate (Figure 4, E and F, lanes 5 and 6). This finding was surprising as the degradation of the peptide when fused to GFP^{NLS} was partially dependent upon Ssa1/Ssa2 in vivo (Supplemental Figure 2). The addition of Ydj1, Hsp104, and Sse1 did not relieve this inhibitory effect (Figure 4, E and F, lanes 7–12).

One hypothesis for this result is that San1 and Ssa1 bind the same exposed hydrophobic sequence and thus compete with each other. To identify potential Ssa1-binding sites, the peptide sequence was analyzed using BiPPred, which is an algorithm that identifies Hsp70-binding sequences (Schneider *et al.*, 2016). Although three sequence stretches were predicted to have affinity for Hsp70, the strongest Hsp70-binding region in the peptide is the same FFLVLIV sequence recognized by San1 (Figure 4G; Fredrickson *et al.*, 2013a). We find it interesting that the same inhibitory effect was not observed in the denatured luciferase assay (Figure 4, C and D). Luciferase has ~20 predicted Hsp70-binding sites (Figure 4H), and it is possible that competition between San1 and Ssa1 for denatured luciferase is considerably reduced due to the many more binding sites that are available in denatured luciferase than the peptide sub-

strate. We consider this and other possibilities in the *Discussion* for the different effects of chaperone addition in each in vitro ubiquitination assay.

Substrate insolubility correlates with the Ssa1/Ssa2 dependency for San1-substrate degradation

The variable participation for Ssa1/Ssa2 in San1-mediated degradation led us to explore the potential underlying reason(s) for the difference in chaperone involvement. One hypothesis is that the Ssa1/Ssa2 Hsp70 chaperones are involved in nuclear import. We think this is unlikely based on the Figure 1 results where we appended an NLS to drive active nuclear import and observed similar Ssa1/Ssa2 dependency for San1-mediated degradation as previously described (McClellan *et al.*, 2005; Prasad *et al.*, 2010, 2012). In addition, Ssa1/Ssa2-dependent San1 substrates showed no observable changes in nuclear localization in *ssa1Δssa2Δ* cells (Figure 2 and Supplemental Figure 1). A second hypothesis is that chaperones are involved as substrate-recognition factors that deliver substrates to San1 for ubiquitination. We think this possibility is also unlikely because we would have observed that all substrates in Figure 1 shared the same dependency on Ssa1/Ssa2, and we would not have observed chaperone-independent San1-mediated ubiquitination in vitro (Figure 4, C–F; Rosenbaum *et al.*, 2011; Ibarra *et al.*, 2016). A third hypothesis is that chaperones maintain the in vivo solubility of certain substrates to enable San1 recognition if the misfolded proteins are exceptionally aggregation prone. This hypothesis is based on the kinetic-partitioning model wherein a key function for chaperones is to aid in partitioning misfolded proteins between oligomeric aggregates and monomeric states (Kim *et al.*, 2013).

To examine substrate solubility, we performed sedimentation assays on all substrates described in Figure 1 in parent and *ssa1Δssa2Δ* cells (Figure 5, A and B). Sedimentation assays allowed us to determine the relative levels of substrate in the soluble fraction versus the insoluble pellet during differential centrifugation. For substrates that showed some dependency on Ssa1/Ssa2 for their degradation (Figure 1), the level of the substrate increased in the insoluble fraction in *ssa1Δssa2Δ* cells (Figure 5A). By contrast, substrates that were degraded in a Ssa1/Ssa2-independent manner, showed little to no transition of substrate into the insoluble pellet in *ssa1Δssa2Δ* cells (Figure 5B), which is similar to the distribution of the soluble

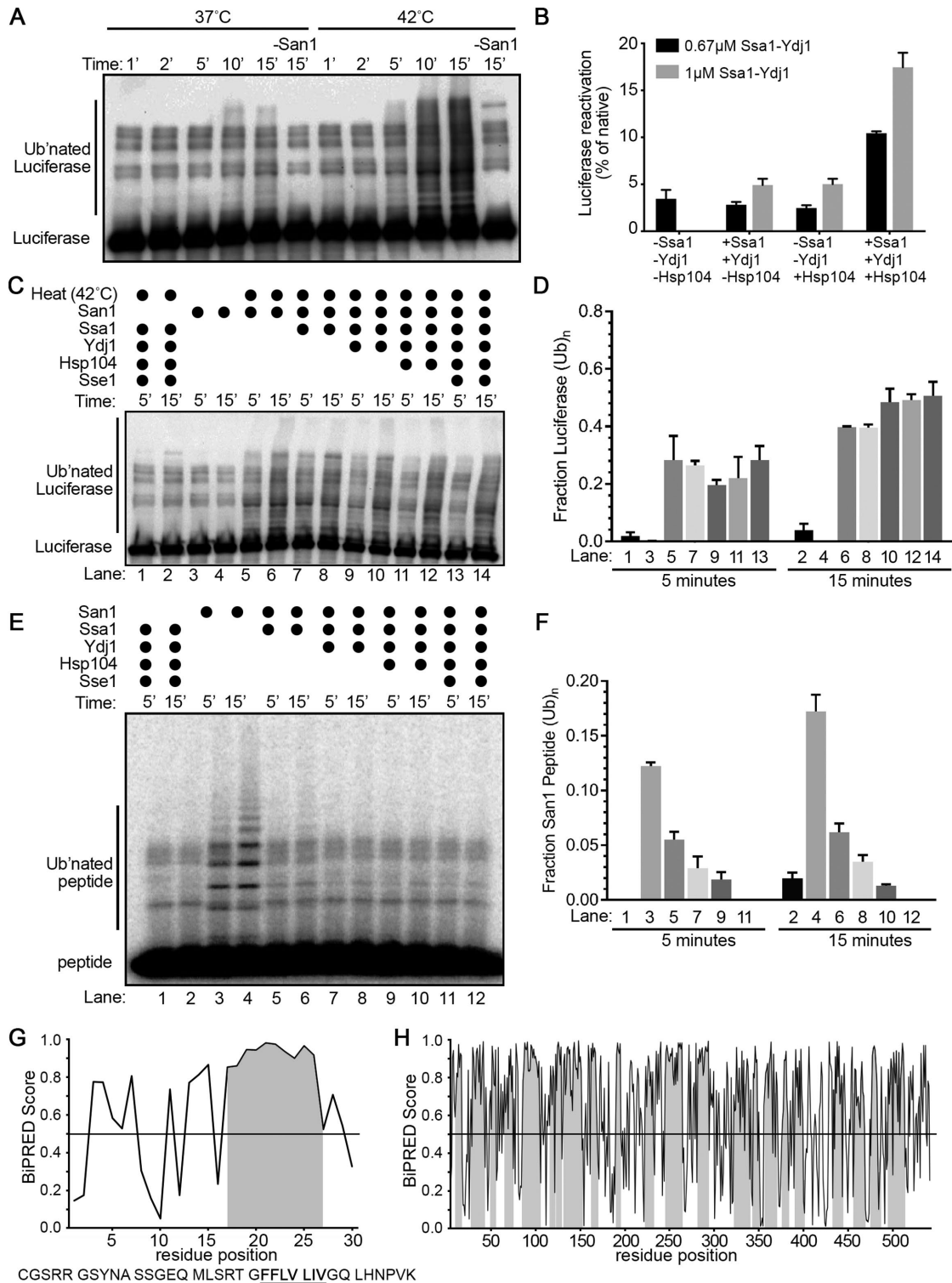


FIGURE 4: Chaperones are dispensable for San1-mediated ubiquitination in vitro. (A) In vitro ubiquitination of luciferase denatured at either 37°C or 42°C. The San1 enzymatic cascade consisted of purified ubiquitin, human ubiquitin-activating enzyme Uba1, yeast Ubc1, and purified San1. Anti-luciferase antibodies were used to detect unmodified and ubiquitinated luciferase. (B) Luciferase renaturation assays were conducted to demonstrate that the chaperones used in the in vitro ubiquitination assays were functional. Luciferase activity was measured by total luminescence and compared with an equivalent amount of native luciferase. The amount of Ssa1-Ydj1 used in the reaction was either 0.167 or 1 μM as indicated. (C) In vitro assays were performed to assess the ubiquitination of denatured luciferase with and without the addition of chaperones. The yeast chaperones Ssa1, Ydj1, Hsp104, and Sse1 were sequentially added to the basic San1 enzymatic cascade as indicated. Reactions were allowed to proceed for 5 or 15 min as indicated above each lane. Luciferase was either present in a native form (lanes 3 and 4) or heat denatured at 42°C (all other lanes). San1 and chaperones were added as indicated above each lane. Anti-luciferase antibodies were used to detect

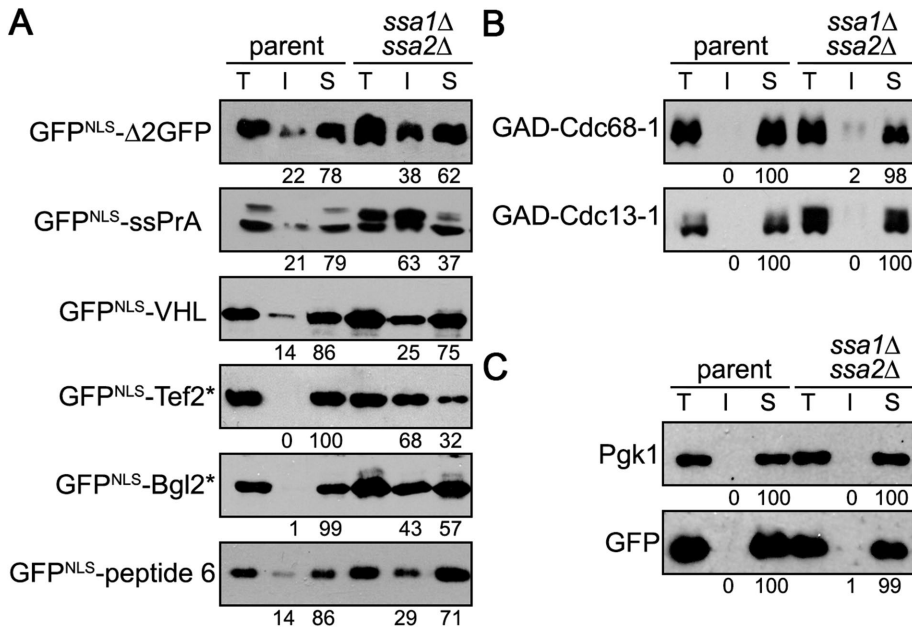


FIGURE 5: Solubility/insolubility assays for substrates that are Ssa1/Ssa2-dependent and independent. Sedimentation assays were performed to determine San1 substrate partitioning between the insoluble pellet fraction (I) and the soluble supernatant (S) in parent and *ssa1Δ/ssa2Δ* cells. Total lysate (T) indicates the total amount of substrate in cell lysates. Anti-GFP, anti-GAD, or anti-Pgk1 antibodies were used to detect each respective substrate. (A) GFP^{NLS}-Δ2GFP, GFP^{NLS}-ΔssPrA, GFP^{NLS}-VHL, GFP^{NLS}-Tef2*, GFP^{NLS}-Bgl2*, and GFP^{NLS}-peptide 6 solubility partitioning. (B) GAD-Cdc68-1 and GAD-Cdc13-1 solubility partitioning. (C) Pgk1 and GFP^{NLS} solubility partitioning. Numbers below each lane represent the insolubility/solubility levels measured with ImageJ from three independently conducted assays.

proteins Pgk1 and GFP^{NLS} (Figure 5C). Thus, there is a correlation between substrate dependency on Ssa1/Ssa2 for degradation and its solubility.

The lack of Ssa1/Ssa2 involvement in San1-mediated degradation is not due to the involvement of other SSA family members

The data gathered thus far indicated that Ssa1/Ssa2 are differentially involved in San1-substrate ubiquitination and degradation (Figures 1 and 3). However, there remains the possibility that other Hsp70 chaperones function in the ubiquitination and degradation of Ssa1/Ssa2-independent San1 substrates. The essential SSA class of Hsp70 chaperones in yeast comprises four SSA paralogues: SSA1, SSA2, SSA3, and SSA4 (Werner-Washburne *et al.*, 1987). The individual members of the SSA Hsp70 chaperones are partially but not completely redundant in terms of substrate activity and expression (Werner-Washburne *et al.*, 1987, 1989; Boorstein and Craig, 1990a,b; Nelson *et al.*, 1992; Sharma *et al.*, 2009). Ssa1 and Ssa2 are expressed constitutively, whereas Ssa3 and Ssa4 are stress-induced variants (Werner-Washburne *et al.*, 1989). It is possible that Ssa3 and

Ssa4 are sufficiently expressed in *ssa1Δssa2Δ* cells in a way that they substitute for Ssa1/Ssa2 in the San1-mediated degradation of Ssa1/Ssa2-independent San1 substrates. To query SSA chaperone redundancy in San1-mediated degradation, we pursued both genetic and pharmacological experiments.

Because the SSA family members are essential for viability, a long-established genetic means to eliminate the function of the SSA class of Hsp70 chaperones is to use the *ssa1-45* strain, in which the SSA2, SSA3, and SSA4 genes have been disrupted by gene insertional mutagenesis and the SSA1 gene has been replaced with a temperature-sensitive allele *ssa1-45* (Becker *et al.*, 1996). Several studies have used this strain to examine the role of the SSA class of Hsp70 chaperones in PQC degradation (Brodsky *et al.*, 1999; Huyer *et al.*, 2004; McClellan *et al.*, 2005; Park *et al.*, 2007; Metzger *et al.*, 2008; Heck *et al.*, 2010; Shiber *et al.*, 2013). When we examined the degradation of GAD-Cdc68-1 and GAD-Cdc13-1 in *ssa1-45* cells, we observed that both San1 substrates were fully stabilized after a 1-h shift to the restrictive temperature of 37°C before the addition of cycloheximide (Figure 6A). Although surprising, the solubility of both substrates was considerably compromised in *ssa1-45* cells at the restrictive temperature (Figure 6B), supporting the idea that the SSA class of Hsp70 chaperones is required for maintaining substrate solubility for San1-mediated degradation.

The difference between the stabilities of GAD-Cdc68-1 and GAD-Cdc13-1 in *ssa1-45* cells versus *ssa1Δssa2Δ* cells was perplexing. It is possible that the difference was due to the assays being conducted at the restrictive temperature of 37°C for the temperature-sensitive *ssa1-45* cells rather than at 30°C for *ssa1Δssa2Δ* cells. Therefore, we reexamined GAD-Cdc68-1 and GAD-Cdc13-1 degradation in *ssa1Δssa2Δ* cells at 37°C, but we did not observe any stabilization at this temperature (Figure 6C). Thus, the differences observed between *ssa1-45* and *ssa1Δssa2Δ* cells cannot be attributed to the temperature alteration in the assay.

An important limitation of the *ssa1-45* strain is that it is chronically deficient in wild-type SSA Hsp70 chaperone function. This impairment could make it appear that SSA Hsp70 chaperones are essential for San1-mediated degradation when the effect might be indirect due to a persistent diminishment in global cellular proteostasis. To avoid the chronic issues of the genetic approach, we explored the role of Hsp70 chaperones in San1-mediated degradation by acute pharmacological inhibition of Hsp70 chaperones with

luciferase. (D) Quantitation of the amount of ubiquitinated luciferase. Data were generated from three independent experiments. (E) *In vitro* ubiquitination assays were performed to assess the ubiquitination of a San1 peptide substrate with and without the addition of chaperones. Radiolabeled San1 peptide was added to reactions in which San1 and chaperones were included as indicated above each lane. Radiolabeled San1 peptide was detected using phosphorimaging. (F) Quantitation of the amount of ubiquitinated peptide. Data was generated from three independent experiments. (G) BiPPred analysis of the peptide sequence for Hsp70-binding sites. Scores greater than 0.5 on the BiPPred scale indicate predicted binding sites for Hsp70. The best predicted site is highlighted with gray. (H) BiPPred analysis of the luciferase sequence for Hsp70-binding sites. Scores over 0.5 on the BiPPred scale indicate predicted binding sites for Hsp70. The best predicted sites are highlighted with gray.

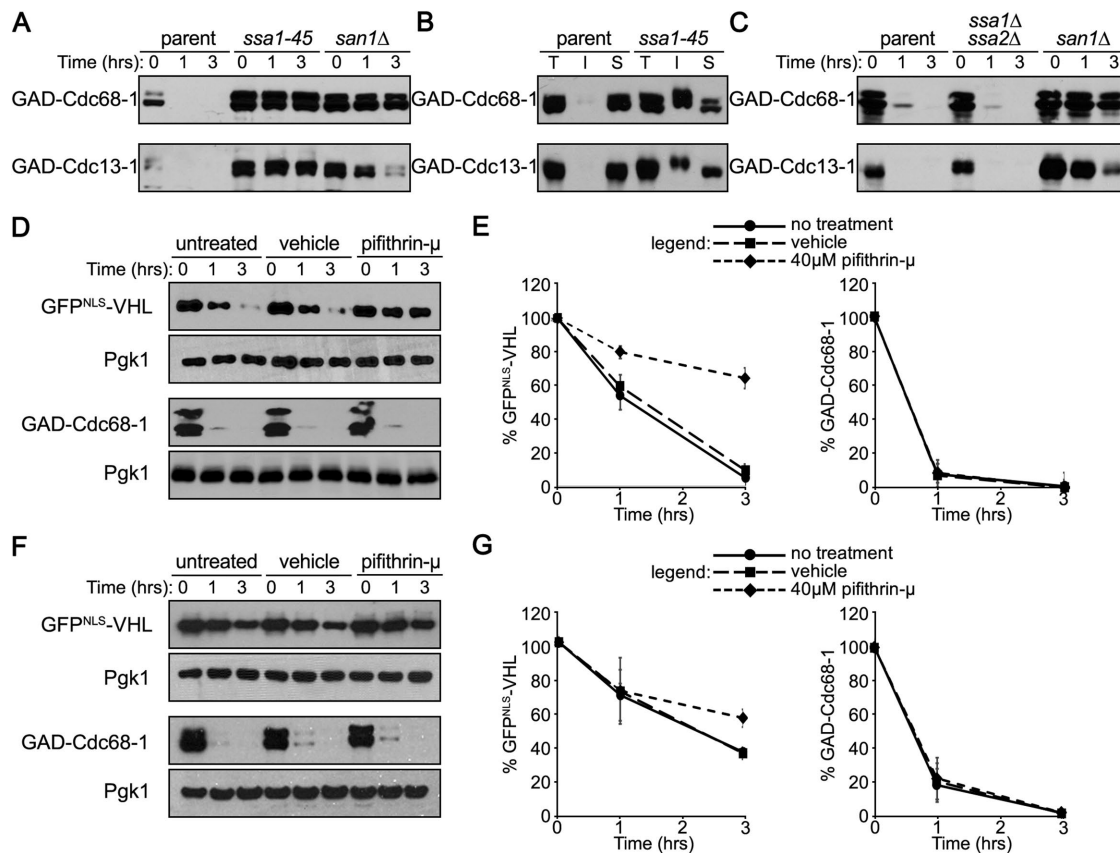


FIGURE 6: SSA class Hsp70 redundancy does not explain the varying involvement of Ssa1/Ssa2 in San1-mediated degradation. (A) Cycloheximide-chase degradation assays were performed on parent, *ssa1-45*, and *san1Δ* cells to assess the stability of Ssa1/Ssa2-independent GAD-Cdc68-1 or GAD-Cdc13-1. Cells were grown at the permissive temperature of 30°C, and then shifted to the restrictive temperature of 37°C for 1 h before cycloheximide addition. Time after cycloheximide addition is indicated above each lane. Anti-GAD antibodies were used to detect each substrate. (B) Sedimentation assays were performed to determine GAD-Cdc68-1 and GAD-Cdc13-1 partitioning between the insoluble pellet fraction (I) and the soluble supernatant (S) in parent and *ssa1-45* cells. Total lysate (T) indicates the total amount of substrate in cell lysates. Anti-GAD antibodies were used to detect each substrate. (C) Cycloheximide-chase degradation assays were performed to assess the stability of GAD-Cdc68-1 and GAD-Cdc13-1 at 37°C in parent, *ssa1Δssa2Δ*, and *san1Δ* cells. Time after cycloheximide addition is indicated above each lane. Anti-GAD antibodies were used to detect each substrate. (D) Addition of pifithrin-μ stabilized the Ssa1/Ssa2-dependent substrate GFP^{NLS}-VHL but not the Ssa1/Ssa2-independent substrate GAD-Cdc68-1 in parent cells. The experiment was performed as in Figure 1A, except pifithrin-μ was added 1 h before cycloheximide addition. Anti-GFP and anti-GAD antibodies were used to detect each respective substrate. Anti-Pgk1 antibodies were used to assess loading. (E) Decay curves for the degradation assays in D. Band intensities were measured using ImageJ with the levels in the 0 time points for each replicate arbitrarily set to 100%. Standard deviation in each graph was determined from three independent assays. (F) Addition of pifithrin-μ stabilized the Ssa1/Ssa2-dependent substrate GFP^{NLS}-VHL but not the Ssa1/Ssa2-independent substrate GAD-Cdc68-1 in *ssa1Δssa2Δ* cells. The experiment was performed as in Figure 1A, except pifithrin-μ was added 1 h before cycloheximide addition. Anti-GFP and anti-GAD antibodies were used to detect each respective substrate. Anti-Pgk1 antibodies were used to assess loading. (G) Decay curves for the degradation assays in F. Band intensities were measured using ImageJ with the levels in the 0 time points for each replicate arbitrarily set to 100%. Standard deviation in each graph was determined from three independent assays.

pifithrin-μ (2-phenylethanesulfonamide), which is a general inhibitor of Hsp70 chaperones (Leu *et al.*, 2009) that is active in yeast (Roy *et al.*, 2015).

We examined how degradation was affected by Hsp70 inhibition using the Ssa1/Ssa2-dependent substrate GFP^{NLS}-VHL and the Ssa1/Ssa2-independent substrate GAD-Cdc68-1. Treatment of parent cells with pifithrin-μ resulted in stabilization of GFP^{NLS}-VHL but not GAD-Cdc68-1 (Figure 6, D and E), consistent with the results observed in *ssa1Δssa2Δ* cells (Figure 1). A key possibility is that there remained sufficient SSA Hsp70 activity in parent cells after the addition of pifithrin-μ that allowed GAD-Cdc68-1 degradation. There-

fore, we examined the degradation of GFP^{NLS}-VHL and GAD-Cdc68-1 in *ssa1Δssa2Δ* cells treated with pifithrin-μ. Because GFP^{NLS}-VHL is already stabilized in *ssa1Δssa2Δ* cells (Figure 1), we anticipated that not much further stabilization would occur by an addition of pifithrin-μ. As expected, we observed modest stabilizing effects on GFP^{NLS}-VHL degradation at the 3-h time point, indicating that there is still some residual Hsp70 activity for GFP^{NLS}-VHL degradation in *ssa1Δssa2Δ* cells (Figure 6, F and G). We did not observe any stabilizing effects of pifithrin-μ on GAD-Cdc68-1 degradation in *ssa1Δssa2Δ* cells (Figure 6, F and G), consistent with GAD-Cdc68-1 degradation being independent of Hsp70 function. Altogether,

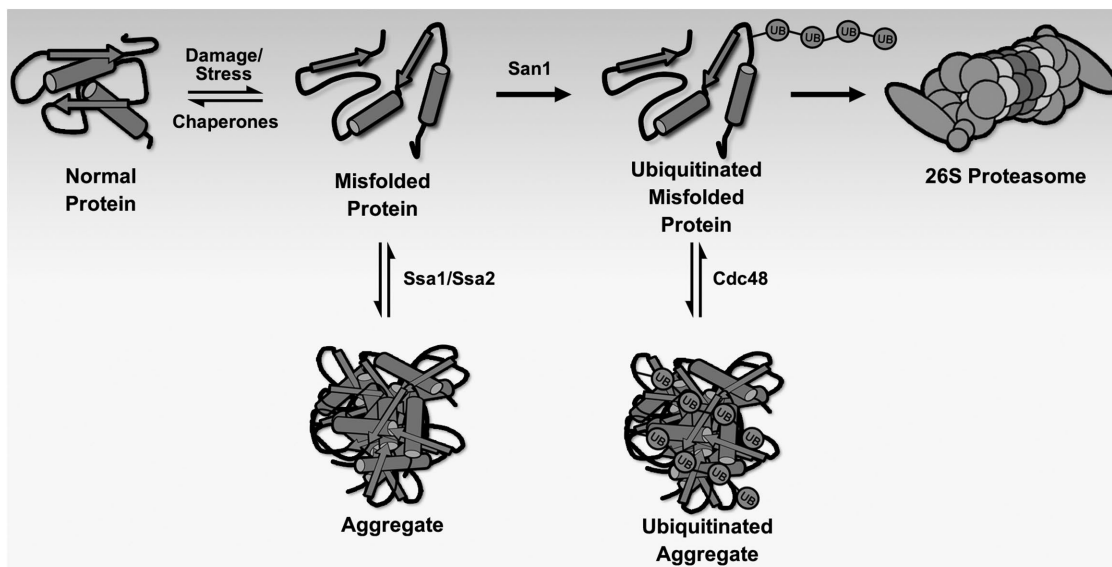


FIGURE 7: Model proposing action of Hsp70 chaperones in the San1 pathway. We propose from the work presented here that the yeast Hsp70 chaperones Ssa1/Ssa2 function to maintain solubility or reverse aggregation of highly aggregation-prone proteins for San1 recognition. This is similar to previous work demonstrating that Cdc48/p97 has a similar role downstream from San1 to facilitate the proteasomal recognition of highly aggregation-prone substrates ubiquitinated by San1 (Gallagher *et al.*, 2014).

acute pharmacological inhibition of Hsp70 chaperones mirrors our fundamental observations in *ssa1Δssa2Δ* cells. In some cases, Hsp70 chaperones are required for San1-mediated ubiquitination and degradation. In other cases, Hsp70 chaperones are dispensable for San1-mediated ubiquitination and degradation.

DISCUSSION

Chaperones are central players in PQC. Although chaperones have been shown to be involved in nuclear PQC degradation, their broad necessity and functional roles have not been fully elucidated. We chose to explore this important aspect of chaperone function because, while our previous studies support that chaperones are not essential for San1-mediated degradation in the nucleus (Rosenbaum *et al.*, 2011), other reports indicated that chaperones are necessary (Heck *et al.*, 2010; Prasad *et al.*, 2010, 2012; Guerriero *et al.*, 2013). Here, we find that the Hsp70 chaperones Ssa1/Ssa2 are important *in vivo* for San1-mediated ubiquitination and degradation in a manner that depends on substrate characteristics. *In vitro*, chaperones have little effect on and, in some cases, are inhibitory for San1-mediated ubiquitination. On the basis of the data presented here and on our previous data where we established *in vivo* interactions between San1 and its substrates but not with Hsp70 chaperones (Rosenbaum *et al.*, 2011), we propose a model in which chaperones act before San1 ubiquitination to maintain misfolded protein solubility in order to enable exposed hydrophobicity recognition by San1 (Figure 7). This varying involvement of Hsp70 chaperones is reminiscent of what we observed with the segregase Cdc48/p97, which appears to maintain solubility for ubiquitinated substrates en route from San1 to the proteasome (Gallagher *et al.*, 2014).

Prior PQC degradation studies have utilized the *ssa1-45* yeast strain (Brodsky *et al.*, 1999; Hoyer *et al.*, 2004; McClellan *et al.*, 2005; Park *et al.*, 2007; Metzger *et al.*, 2008; Heck *et al.*, 2010; Shiber *et al.*, 2013), which has been genetically ablated for the function of the essential SSA class of Hsp70 chaperones (Werner-Washburne *et al.*, 1987). We think there are important limitations to the *ssa1-45* strain that should be considered before interpretation of Hsp70

PQC degradation effects observed solely in the *ssa1-45* strain. For example, inactivation of SSA2 in the *ssa1-45* strain occurred by insertional mutagenesis wherein the first 306 residues of Ssa2 can still be expressed (Craig and Jacobsen, 1984). Inactivation of SSA3 and SSA4 was also achieved by insertional mutagenesis with the potential for N-terminal fragments of each protein also to be expressed (Werner-Washburne *et al.*, 1987). At the restrictive temperature of 37°C, expression of these fragments will be increased due to up-regulated expression of the SSA genes at elevated temperatures (Werner-Washburne *et al.*, 1989; Gasch *et al.*, 2000). Production of SSA chaperone fragments is salient as San1 appears to be rate-limiting in the cell, reflected by the observation that increased misfolded protein expression can slow the degradation of individual San1 substrates (Heck *et al.*, 2010). In many cases, results using the *ssa1-45* strain may accurately reflect a key role for the SSA Hsp70 chaperones in PQC degradation. In other cases, the results might be misleading due to potential indirect effects. Therefore, we suggest that care should be taken when interpreting results about SSA Hsp70 chaperone requirement in PQC degradation if the *ssa1-45* strain is the sole means used to determine involvement of these chaperones. Regardless, we do establish here that Ssa1/Ssa2 play a role in the nuclear PQC degradation of some misfolded proteins.

The *in vitro* assay was illuminating in terms of chaperone function for San1-mediated ubiquitination. We saw no effect for chaperones enhancing San1 activity. We did observe the surprising result that the addition of chaperones inhibited the San1-mediated ubiquitination for the peptide substrate. Why is there a difference between luciferase and the peptide substrate in terms of chaperone effects *in vitro*? First, it is possible that the peptide substrate contains a sequence motif that chaperones bind with higher affinity than San1, whereas denatured luciferase may interact less strongly with chaperones than with San1. This scenario incorporates the possibility for chaperones to bind the peptide substrate and outcompete San1 for binding, but allow denatured luciferase to be sufficiently free for San1 to bind. Second, it is possible that competition between San1 and Ssa1 for denatured luciferase may be considerably reduced due to the

Yeast strain	Genotype	Reference
JB67	<i>his3-11,15, leu2-3112, ura3-52, trp1Δ1, lys2, ssa1-45, ssa2-1, ssa3-1, ssa4-2</i>	Becker et al., 1996
JN516	<i>his3-11,15, leu2-3112, ura3-52, trp1Δ1, lys2, SSA1, ssa2-1, ssa3-1, ssa4-2</i>	Becker et al., 1996
RGY5113	W303a <i>san1Δ</i>	This study
RGY5739	RGY5113 <i>NUP60::mCherry::HIS3</i>	This study
RGY5983	W303a <i>NUP60::mCherry::HIS3</i>	This study
RGY5984	RPY283 <i>NUP60::mCherry::HIS3</i>	This study
RPY283	W303a <i>ssa1Δ ssa2Δ</i>	Prasad et al., 2010
W303a	<i>ade2-1 his3-11 ura3-1 trp1-1 leu2-3 can1-100</i>	Prasad et al., 2010

Plasmid	Description	Reference
pRG1289	GFP ^{NLS} -Tef2*, <i>LEU2</i> , 2 μm	Rosenbaum et al., 2011
pRG1290	GFP ^{NLS} -Bgl2*, <i>LEU2</i> , 2 μm	Rosenbaum et al., 2011
pRG1291	GFP ^{NLS} -peptide 6, <i>LEU2</i> , 2 μm	Fredrickson et al., 2011
pRG2054	GAD-Cdc68-1, <i>LEU2</i> , 2 μm	Rosenbaum et al., 2011
pRG2056	GAD-Cdc13-1, <i>LEU2</i> , 2 μm	Rosenbaum et al., 2011
pRG3027	GFP ^{NLS} -VHL, <i>URA3</i> , 2 μm	This study
pRG4141	GFP ^{NLS} -Δ2GFP, <i>HIS3</i> , YCp	This study
pRG4142	GFP ^{NLS} -ΔssPrA, <i>HIS3</i> , YCp	This study
pRG4263	GFP ^{NLS} -San1 peptide, <i>LEU2</i> , Ylp	This study

TABLE 1: Yeast strains and plasmids used in this study.

likelihood of additional binding sites that are available in denatured luciferase than the peptide substrate (Figure 4, G and H). Third, it is possible that Ssa1 binds San1 and inhibits San1's ability to recognize the peptide. We think this latter scenario is unlikely in that binding of Ssa1 to San1 in an inhibitory manner should have also reduced ubiquitination of denatured luciferase *in vitro*, which we did not observe.

Although the *in vitro* assays demonstrate that chaperones are dispensable for San1-substrate ubiquitination, we consider a more nuanced stance that Hsp70 chaperones become necessary *in vivo* when misfolded proteins aggregate and exceed the capacity of San1 to bind and ubiquitinate the monomeric forms of its substrates. Misfolded proteins can exist on a spectrum of monomeric, oligomeric, largely aggregated, and observable cellular inclusions *in vivo* (Hartl et al., 2011; Hartl, 2017). The *in vivo* rates of partitioning to monomeric states that are recognizable by San1 will likely dictate not only the speed of substrate ubiquitination and degradation, but also the necessity of chaperones to facilitate partitioning the misfolded substrate to accessible forms. In this regard, the aggregation propensity of the substrate would be a key determinant for chaperone involvement in San1-mediated nuclear PQC degradation. A faster rate of aggregation for a misfolded protein could result in a greater dependency on Hsp70 chaperones for San1-mediated degradation. Real-time *in vivo* assays to monitor partitioning of a misfolded protein between each of its states will need to be developed to further define the parameters of chaperone involvement in a misfolded protein's nuclear PQC degradation.

We have presented data for the SSA class of Hsp70 chaperones and how they are involved in nuclear PQC degradation. It is also worth considering how other chaperones might operate in the clearance of nuclear misfolded proteins. There is evidence in the literature that other Hsp40 and Hsp110 chaperones could be involved (Heck et al., 2010; Prasad et al., 2010, 2012, 2018; Brower et al., 2013; Guerriero et al., 2013). How these chaperones function to facilitate nuclear PQC degradation remains an area of active study,

though facilitating nuclear import is one observed role (Miller et al., 2015; Prasad et al., 2018). We hope our work here inspires future studies to reveal the mechanism of other chaperones in nuclear PQC degradation.

MATERIALS AND METHODS

Yeast strains and plasmids

Yeast strains and plasmids used in this study are listed in Table 1. Plasmid sequences and cloning details will be provided upon request.

Degradation assays

Cycloheximide-chase degradation assays were performed similarly to previously described (Fredrickson et al., 2011). Cells were grown in liquid synthetic media with 3% raffinose or glucose to $\sim 1 \times 10^7$ cells/ml. Galactose was added to 3% and the cells were incubated for 3 h. In the case of drug addition, cells were treated with 40 μM pifithrin-μ (2-phenylethanesulfonamide; Sigma) for 1 h before cycloheximide addition. We note that pifithrin-μ is labile in dimethyl sulfoxide over time, and care should be taken to use freshly prepared stocks. Furthermore, some strains (JB67 and JN5177) appear to be refractory to pifithrin-μ. In the case of the temperature-sensitive *ssa1-45* strain, cells were shifted to 37°C for 1 h before cycloheximide addition. To initiate the degradation studies, cycloheximide was added to 50 μg/ml and the cells further incubated for 0–3 h. Cells were lysed at the appropriate time point in 200 μl SUMEB buffer (1% SDS, 8 M urea, 10 mM MOPS [3-(*N*-morpholino)propanesulfonic acid], pH 6.8, 10 mM EDTA, 0.01% bromophenol blue, 1 mM phenylmethylsulfonyl fluoride [PMSF]) by vortexing with 100 μl of 0.5 mm acid-washed glass beads (Biospec Products). Proteins were resolved on 8% or 16% SDS-PAGE gels, transferred to nitrocellulose, and immunoblotted with anti-GFP antibodies (Sigma) or anti-Gal4AD (GAD) antibodies (Millipore) for substrate detection, and anti-Pgk1 antibodies (Sigma) to assess loading. All experiments

were performed a minimum of three times with at least two biological replicates.

Solubility assays

Solubility assays were performed similarly to previously described (Fredrickson *et al.*, 2013b). Briefly, cells were grown in culture to $\sim 1 \times 10^7$ cells/ml. Cells (4 ml) were collected and lysed in lysis buffer (100 mM Tris-HCl, pH 7.5, 200 mM NaCl, 1 mM EDTA, 1 mM dithiothreitol [DTT], 5% glycerol, and 0.1% Nonidet P40) + PMSF (phenylmethylsulfonyl fluoride) by vortexing 5 min at 4°C with 100 μ l of 0.5 mm acid-washed glass beads. Unlysed cells were removed from lysates by centrifugation at $700 \times g$ for 1 min at 4°C. Lysate (50 μ l), which represents the “total lysate,” was removed and added to 50 μ l SUMEB. The remaining lysate was centrifuged at $12,800 \times g$ for 15 min at 4°C. Supernatant (100 μ l), which represents the “soluble fraction,” was added to 100 μ l SUMEB. The pellet, which represents the “insoluble fraction,” was resuspended in 100 μ l lysis buffer and 100 μ l SUMEB. Samples were incubated at 65°C for 5 min and clarified for 5 min by centrifugation at $12,800 \times g$. Proteins were resolved on 8% or 16% SDS–PAGE gels, 4–12% or 4–20% Tris-glycine gradient gels (Lonza), transferred to nitrocellulose, and immunoblotted with anti-GFP antibodies, anti-Gal4AD (GAD) antibodies, or anti-Pgk1 antibodies. All experiments were performed a minimum of three times with at least two biological replicates.

Microscopy

Cells were grown in 3% raffinose media to $\sim 0.8 \times 10^7$ cells/ml. Galactose was added to 3% and the cells incubated 6 h. Cells were harvested, fixed in 4% paraformaldehyde in 0.1 M sucrose for 15 min, washed in wash buffer (1.2 M sorbitol, 0.4 M KPO₄), stained with DAPI (4',6-diamidino-2-phenylindole) for 10 min in wash buffer plus 2% Triton X-100, and washed two times in wash buffer. Cells were imaged at room temperature on a Nikon Eclipse 90i with a 100 \times objective, filters for GFP (HC HiSN Zero Shift filter set with excitation wavelength, 450–490 nm; dichroic mirror, 495 nm; and emission filter, 500–550 nm) or DAPI (HC HiSN Zero Shift filter set with excitation wavelength, 325–375 nm; dichroic mirror, 400 nm; and emission filter, 435–485 nm), and a Photometrics Cool Snap HQ2 cooled CCD camera with NIS-Elements acquisition software. All images were subsequently processed using Adobe Photoshop CC 2017. All experiments were performed a minimum of three times with at least two biological replicates.

In vivo ubiquitination assays

Cells were grown in 3% raffinose medium to $\sim 1 \times 10^7$ cells/ml. Galactose was added to 3% and the cells were incubated for 3 h. Harvested cells were lysed in 1 ml lysis buffer (50 mM Tris, pH 7.5, 150 mM NaCl, 1 mM EDTA, 10% glycerol, 1% NP-40, 100 mM PMSF, and 10 mM NEM [*N*-ethylmaleimide]). Lysates were clarified by centrifugation, and 20 μ l anti-ubiquitin TUBE agarose beads (LifeSensors) was added to lysates and incubated overnight at 4°C. The beads were washed four times with 1 ml lysis buffer (without NEM). Affinity purified proteins were eluted from the beads using 25 μ l SUMEB buffer. All samples were incubated at 65°C for 10 min. Proteins were resolved on 8% or 16% SDS–PAGE gels, transferred to nitrocellulose, and immunoblotted with anti-GFP antibodies or anti-GAD antibodies. All experiments were performed a minimum of three times.

Chaperone purification

Saccharomyces cerevisiae Hsp104 was expressed from the pNOTAG-Hsp104 vector (Hattendorf and Lindquist, 2002) and purified as previ-

ously described (Desantis *et al.*, 2014; Torrente *et al.*, 2016). Briefly, pNOTAG-Hsp104 was used to transform BL21(DE3) RIL *E. coli*. Transformed cells were grown in 2xYT broth supplemented with 25 μ g/ml chloramphenicol and 100 μ g/ml ampicillin at 37°C until an OD₆₀₀ of 0.4–0.6 was reached, at which point cells were cooled to 15°C. Expression was induced by the addition of 1 mM isopropyl 1-thio- β -D-galactopyranoside for 15–18 h at 15°C. Cells were harvested by centrifugation ($4000 \times g$, 4°C, 25 min), resuspended in lysis buffer (50 mM Tris-HCl, pH 8.0, 10 mM MgCl₂, 2.5% glycerol, 2 mM β -mercaptoethanol, 5 μ M pepstatin, cOmplete EDTA-free protease inhibitors [Roche]). Cells were treated on ice with 20 mg lysozyme per 1 l culture and lysed by sonication. Cell debris was removed by centrifugation at $30,000 \times g$ at 4°C for 20 min, and the supernatant was applied to Affi-Gel Blue resin (Bio-Rad). Resin was incubated with the lysates for 4 h at 4°C with slow rotation. Resin was then washed four times with wash buffer (50 mM Tris-HCl, pH 8.0, 10 mM MgCl₂, 100 mM KCl, 2.5% glycerol, 2 mM β -mercaptoethanol). Hsp104 was eluted with wash buffer supplemented with 1 M KCl. The protein was exchanged into running buffer Q (20 mM Tris-HCl, pH 8.0, 0.5 mM EDTA, 5 mM MgCl₂, 50 mM NaCl), further purified by ResourceQ anion exchange chromatography, and eluted with a linear salt gradient (50 mM–1 M NaCl). Eluted protein was then exchanged into storage buffer (40 mM HEPES-KOH, pH 7.4, 500 mM KCl, 20 mM MgCl₂, 50% glycerol, 1 mM DTT), snap-frozen, and stored at –80°C until use.

Saccharomyces cerevisiae Ssa1, Ydj1, and Sse1 (in pE-SUMOpro; Life Sensors) were purified as described (Michalska *et al.*, 2019). Briefly, Ssa1, Ydj1, and Sse1 were expressed as N-terminally His₆-SUMO-tagged proteins in BL21(DE3) RIL cells. Transformed cells were grown at 37°C in Luria broth supplemented with 25 μ g/ml chloramphenicol and 100 μ g/ml ampicillin to an OD₆₀₀ ~0.5. Cultures were cooled to 15°C, and expression was induced with 1 mM IPTG (isopropyl β -D-1-thiogalactopyranoside) for 16 h at 15°C. Cells were harvested, resuspended in lysis buffer (50 mM HEPES, pH 7.5, 750 mM KCl, 5 mM MgCl₂, 10% glycerol, 20 mM imidazole, 2 mM β -mercaptoethanol, 5 μ M pepstatin A, and cOmplete protease inhibitor [Roche]), and lysed by treatment with lysozyme and sonication. Lysates were clarified by centrifugation ($16,000 \times g$, 20 min, 4°C), and incubated with Ni-NTA resin for 90 min at 4°C. Resin was washed with 10 column volumes of wash buffer (50 mM HEPES, pH 7.5, 750 mM KCl, 10 mM MgCl₂, 10% glycerol, 20 mM imidazole, 1 mM ATP, 2 mM β -mercaptoethanol) and eluted with two column volumes of elution buffer (wash buffer with 300 mM imidazole). To cleave the His₆-SUMO tag, Ulp1 was added at a 1:100 M ratio, and imidazole was removed by dialysis against wash buffer. After dialysis, protein was loaded onto a 5 ml HisTrap column (GE Healthcare) and eluted with a linear imidazole gradient (20–350 mM) over 40 column volumes. Fractions containing cleaved protein were pooled, concentrated, and purified further by Resource Q ion exchange chromatography.

In vitro ubiquitination assays

In vitro luciferase ubiquitination reactions were performed in a reaction buffer containing 30 mM Tris-HCl, pH 7.5, 5 mM MgCl₂, 5 mM ATP, 2 mM DTT, and 100 mM NaCl with an ATP-regenerating system containing 1 mM creatine phosphate (VWR) and 0.25 μ M creatine kinase (Sigma Aldrich). Ubiquitin (Boston Biochem; 60 μ M), human ubiquitin-activating enzyme (1 μ M), yeast ubiquitin-conjugating enzyme Ubc1 (10 μ M), purified San1 (with all Lys residues changed to Arg; 0.5 μ M), and the indicated combinations of chaperones Ssa1, Ydj1, and Hsp104 (1 μ M) were first incubated for 2 min. Firefly luciferase (Sigma Aldrich; 0.5 μ M) was then added as the reactions were heated to 42°C. Time points were quenched in SDS–PAGE loading

buffer and ubiquitinated products were separated on 4–20% SDS–PAGE gels (Lonza). Substrate and products were transferred to nitrocellulose and immunoblotted with anti-luciferase antibodies (Sigma).

In vitro San1 peptide ubiquitination reactions were performed using a peptide (50 μ M) that was radiolabeled in the presence of γ -³²P labeled ATP (Perkin Elmer) and cAMP-dependent protein kinase (New England Biolabs) for 1 h at 30°C in a buffer provided by the manufacturer that had been supplemented with 0.1% Tween-20 (Ibarra *et al.*, 2016). All reactions were carried out in the same reaction buffer used for luciferase reactions (also supplemented with 0.1% Tween-20) and an ATP-regenerating system as described above for luciferase ubiquitination. Human ubiquitin-activating enzyme (1 μ M), yeast ubiquitin-conjugating enzyme Ubc1 (10 μ M), purified San1 (with all Lys residues changed to Arg, 0.5 μ M), and the indicated combinations of chaperones Ssa1, Ydj1, and Hsp104 (1 μ M) were sequentially added to 1.5 ml Eppendorf tubes. Radiolabeled San1 peptide (5 μ M) was then added to initiate the reactions. Time points were quenched in SDS–PAGE loading buffer, and both substrate and ubiquitinated products were separated on 4–20% SDS–PAGE gels (Lonza). Gels were dried and exposed to a phosphor screen before imaging on a Typhoon 9410. Quantitation of substrate and products was performed using ImageQuant (GE Healthcare).

Luciferase reactivation assays

The luciferase reactivation assay was performed similarly as previously described (Sweeny *et al.*, 2015). A solution containing 0.1 μ M luciferase was heated at 45°C for 15 min and then diluted 20-fold into the reaction mix. The reaction mix contained an ATP-regenerating system (5 mM ATP, 10 mM phosphocreatine, and 0.1 mM creatine kinase), denatured luciferase, 1 μ M monomeric Hsp104, 0.167 or 1 μ M of Ssa1-Ydj1 each as indicated in the figures. The assays were incubated for 90 min at 25°C. At the end of the reaction, luciferase activity was assessed with a luciferase assay system (Promega). Recovered luminescence was monitored using a Tecan Infinite M1000 plate reader and compared with an equivalent amount of undenatured, native luciferase.

Image processing

Western blots were scanned using an Epson Perfection V350 Photo scanner at 300 dpi. Images were processed with an iMac or Pro computer (Apple) using Photoshop (Adobe). Degradation, ubiquitination, and solubility data were quantified using ImageJ (<https://imagej.nih.gov/ij/>).

ACKNOWLEDGMENTS

We thank Pamela Gallagher, Janani Gopalan, Sarah Clowes-Candadai, and Grace Woodruff for experimental assistance throughout the years of this study. We also gratefully thank Jeff Brodsky and Davis Ng for yeast strains and plasmids. This work was supported by National Institutes of Health/National Institute of General Medical Sciences (NIH/NIGMS) training grant no. 5T32GM-007750 (R.D.J. and E.K.F.), NIH/National Institute on Aging Grant no. R01AG-031136 (R.G.G.), NIH/NIGMS Grants no. P20GM-103440 and no. R15GM-117555 (G.K.), and National Science Foundation–US–Israeli Binational Science Foundation Grant no. 1714468 (R.G.G., T.R.).

REFERENCES

Ballinger CA, Connell P, Wu Y, Hu Z, Thompson LJ, Yin LY, Patterson C (1999). Identification of CHIP, a novel tetratricopeptide repeat-containing protein that interacts with heat shock proteins and negatively regulates chaperone functions. *Mol Cell Biol* 19, 4535–4545.

Becker J, Walter W, Yan W, Craig EA (1996). Functional interaction of cytosolic hsp70 and a DnaJ-related protein, Ydj1p, in protein translocation in vivo. *Mol Cell Biol* 16, 4378–4386.

Boorstein WR, Craig EA (1990a). Structure and regulation of the SSA4 HSP70 gene of *Saccharomyces cerevisiae*. *J Biol Chem* 265, 18912–18921.

Boorstein WR, Craig EA (1990b). Transcriptional regulation of SSA3, an HSP70 gene from *Saccharomyces cerevisiae*. *Mol Cell Biol* 10, 3262–3267.

Brodsky JL, Werner ED, Dubas ME, Goeckeler JL, Kruse KB, McCracken AA (1999). The requirement for molecular chaperones during endoplasmic reticulum-associated protein degradation demonstrates that protein export and import are mechanistically distinct. *J Biol Chem* 274, 3453–3460.

Brower CS, Piatkov KI, Varshavsky A (2013). Neurodegeneration-associated protein fragments as short-lived substrates of the N-end rule pathway. *Mol Cell* 50, 161–171.

Chen B, Retzlaff M, Roos T, Frydman J (2011). Cellular strategies of protein quality control. *Cold Spring Harb Perspect Biol* 3, a004374.

Craig EA, Jacobsen K (1984). Mutations of the heat inducible 70 kilodalton genes of yeast confer temperature sensitive growth. *Cell* 38, 841–849.

Denic V, Quan EM, Weissman JS (2006). A luminal surveillance complex that selects misfolded glycoproteins for ER-associated degradation. *Cell* 126, 349–359.

Desantis ME, Sweeny EA, Snead D, Leung EH, Go MS, Gupta K, Wendler P, Shorter J (2014). Conserved distal loop residues in the Hsp104 and ClpB middle domain contact nucleotide-binding domain 2 and enable Hsp70-dependent protein disaggregation. *J Biol Chem* 289, 848–867.

Eisele F, Wolf DH (2008). Degradation of misfolded protein in the cytoplasm is mediated by the ubiquitin ligase Ubr1. *FEBS Lett* 582, 4143–4146.

Evans DR, Brewster NK, Xu Q, Rowley A, Altheim BA, Johnston GC, Singer RA (1998). The yeast protein complex containing cdc68 and pob3 mediates core-promoter repression through the cdc68 N-terminal domain. *Genetics* 150, 1393–1405.

Fredrickson EK, Clowes Candadai SV, Tam CH, Gardner RG (2013a). Means of self-preservation: how an intrinsically disordered ubiquitin-protein ligase averts self-destruction. *Mol Biol Cell* 24, 1041–1052.

Fredrickson EK, Gallagher PS, Clowes Candadai SV, Gardner RG (2013b). Substrate recognition in nuclear protein quality control degradation is governed by exposed hydrophobicity that correlates with aggregation and insolubility. *J Biol Chem* 288, 6130–6139.

Fredrickson EK, Gardner RG (2012). Selective destruction of abnormal proteins by ubiquitin-mediated protein quality control degradation. *Semin Cell Dev Biol* 23, 530–537.

Fredrickson EK, Rosenbaum JC, Locke MN, Milac TI, Gardner RG (2011). Exposed hydrophobicity is a key determinant of nuclear quality control degradation. *Mol Biol Cell* 22, 2384–2395.

Gallagher PS, Clowes Candadai SV, Gardner RG (2014). The requirement for Cdc48/p97 in nuclear protein quality control degradation depends on the substrate and correlates with substrate insolubility. *J Cell Sci* 127, 1980–1991.

Gardner RG, Nelson ZW, Gottschling DE (2005). Degradation-mediated protein quality control in the nucleus. *Cell* 120, 803–815.

Gasch AP, Spellman PT, Kao CM, Carmel-Harel O, Eisen MB, Storz G, Botstein D, Brown PO (2000). Genomic expression programs in the response of yeast cells to environmental changes. *Mol Biol Cell* 11, 4241–4257.

Glover JR, Lindquist S (1998). Hsp104, Hsp70, and Hsp40: a novel chaperone system that rescues previously aggregated proteins. *Cell* 94, 73–82.

Guerrero CJ, Weiberth KF, Brodsky JL (2013). Hsp70 targets a cytoplasmic quality control substrate to the San1p ubiquitin ligase. *J Biol Chem* 288, 18506–18520.

Hartl FU (2017). Protein misfolding diseases. *Annu Rev Biochem* 86, 21–26.

Hartl FU, Andreas B, Hayer-Hartl M (2011). Molecular chaperones in protein folding and proteostasis. *Nature* 475.

Hattendorf DA, Lindquist SL (2002). Analysis of the AAA sensor-2 motif in the C-terminal ATPase domain of Hsp104 with a site-specific fluorescent probe of nucleotide binding. *Proc Natl Acad Sci USA* 99, 2732–2737.

Heck JW, Cheung SK, Hampton RY (2010). Cytoplasmic protein quality control degradation mediated by parallel actions of the E3 ubiquitin ligases Ubr1 and San1. *Proc Natl Acad Sci USA* 107, 1106–1111.

Huyer G, Piluek WF, Fansler Z, Kreft SG, Hochstrasser M, Brodsky JL, Michaelis S (2004). Distinct machinery is required in *Saccharomyces cerevisiae* for the endoplasmic reticulum-associated degradation of a multispanning membrane protein and a soluble luminal protein. *J Biol Chem* 279, 38369–38378.

- Ibarra R, Sandoval D, Fredrickson EK, Gardner RG, Kleiger G (2016). The San1 ubiquitin ligase functions preferentially with ubiquitin-conjugating enzyme Ubc1 during protein quality control. *J Biol Chem* 291, 18778–18790.
- Jackrel ME, DeSantis ME, Martinez BA, Castellano LM, Stewart RM, Caldwell KA, Caldwell GA, Shorter J (2014). Potentiated Hsp104 variants antagonize diverse proteotoxic misfolding events. *Cell* 156, 170–182.
- Jiang J, Ballinger CA, Wu Y, Dai Q, Cyr DM, Hohfeld J, Patterson C (2001). CHIP is a U-box-dependent E3 ubiquitin ligase: identification of Hsc70 as a target for ubiquitylation. *J Biol Chem* 276, 42938–42944.
- Kim YE, Hipp MS, Bracher A, Hayer-Hartl M, Ulrich Hartl F (2013). Molecular chaperone functions in protein folding and proteostasis. *Annu Rev Biochem* 82, 323–355.
- Leu JI, Pimkina J, Frank A, Murphy ME, George DL (2009). A small molecule inhibitor of inducible heat shock protein 70. *Mol Cell* 36, 15–27.
- McClellan AJ, Scott MD, Frydman J (2005). Folding and quality control of the VHL tumor suppressor proceed through distinct chaperone pathways. *Cell* 121, 739–748.
- Metzger MB, Maurer MJ, Dancy BM, Michaelis S (2008). Degradation of a cytosolic protein requires endoplasmic reticulum-associated degradation machinery. *J Biol Chem* 283, 32302–32316.
- Michalska K, Zhang K, March ZM, Hatzos-Skintges C, Pintilie G, Bigelow L, Castellano LM, Miles LJ, Jackrel ME, Chuang E, et al. (2019). Structure of *Calcarisporiella thermophila* Hsp104 disaggregase that antagonizes diverse proteotoxic misfolding events. *Structure* 27, 449–463.e447.
- Miller SB, Ho CT, Winkler J, Khokhrina M, Neuner A, Mohamed MY, Guilbride DL, Richter K, Lisby M, Schiebel E, et al. (2015). Compartment-specific aggregates direct distinct nuclear and cytoplasmic aggregate deposition. *EMBO J* 34, 778–797.
- Murata S, Minami Y, Minami M, Chiba T, Tanaka K (2001). CHIP is a chaperone-dependent E3 ligase that ubiquitylates unfolded protein. *EMBO Rep* 2, 1133–1138.
- Nakatsukasa K, Huyer G, Michaelis S, Brodsky JL (2008). Dissecting the ER-associated degradation of a misfolded polytopic membrane protein. *Cell* 132, 101–112.
- Nelson RJ, Heschl MF, Craig EA (1992). Isolation and characterization of extragenic suppressors of mutations in the SSA hsp70 genes of *Saccharomyces cerevisiae*. *Genetics* 131, 277–285.
- Nillegoda NB, Theodoraki MA, Mandal AK, Mayo KJ, Ren HY, Sultana R, Wu K, Johnson J, Cyr DM, Caplan AJ (2010). Ubr1 and Ubr2 function in a quality control pathway for degradation of unfolded cytosolic proteins. *Mol Biol Cell* 21, 2102–2116.
- Nishikawa SI, Fewell SW, Kato Y, Brodsky JL, Endo T (2001). Molecular chaperones in the yeast endoplasmic reticulum maintain the solubility of proteins for retrotranslocation and degradation. *J Cell Biol* 153, 1061–1070.
- Nugent CI, Hughes TR, Lue NF, Lundblad V (1996). Cdc13p: a single-strand telomeric DNA-binding protein with a dual role in yeast telomere maintenance. *Science* 274, 249–252.
- Park SH, Bolender N, Eisele F, Kostova Z, Takeuchi J, Coffino P, Wolf DH (2007). The cytoplasmic Hsp70 chaperone machinery subjects misfolded and endoplasmic reticulum import-incompetent proteins to degradation via the ubiquitin–proteasome system. *Mol Biol Cell* 18, 153–165.
- Prasad R, Kawaguchi S, Ng DT (2010). A nucleus-based quality control mechanism for cytosolic proteins. *Mol Biol Cell* 21, 2117–2127.
- Prasad R, Kawaguchi S, Ng DT (2012). Biosynthetic mode can determine the mechanism of protein quality control. *Biochem Biophys Res Commun* 425, 689–695.
- Prasad R, Xu C, Ng DTW (2018). Hsp40/70/110 chaperones adapt nuclear protein quality control to serve cytosolic clients. *J Cell Biol* 217, 2019–2032.
- Rosenbaum JC, Fredrickson EK, Oeser ML, Garrett-Engele CM, Locke MN, Richardson LA, Nelson ZW, Hetrick ED, Milac TI, Gottschling DE, Gardner RG (2011). Disorder targets misorder in nuclear quality control degradation: a disordered ubiquitin ligase directly recognizes its misfolded substrates. *Mol Cell* 41, 93–106.
- Roy J, Mitra S, Sengupta K, Mandal AK (2015). Hsp70 clears misfolded kinases that partitioned into distinct quality-control compartments. *Mol Biol Cell* 26, 1583–1600.
- Samant RS, Livingston CM, Sontag EM, Frydman J (2018). Distinct proteostasis circuits cooperate in nuclear and cytoplasmic protein quality control. *Nature* 563, 407–411.
- Schneider M, Rosam M, Glaser M, Patronov A, Shah H, Back KC, Daake MA, Buchner J, Antes I (2016). BiPPred: combined sequence- and structure-based prediction of peptide binding to the Hsp70 chaperone BiP. *Proteins* 84, 1390–1407.
- Sharma D, Martineau CN, Le Dall MT, Reidy M, Masison DC, Kabani M (2009). Function of SSA subfamily of Hsp70 within and across species varies widely in complementing *Saccharomyces cerevisiae* cell growth and prion propagation. *PLoS One* 4, e6644.
- Shiber A, Breuer W, Brandeis M, Ravid T (2013). Ubiquitin conjugation triggers misfolded protein sequestration into quality control foci when Hsp70 chaperone levels are limiting. *Mol Biol Cell* 24, 2076–2087.
- Sweeny EA, Jackrel ME, Go MS, Sochor MA, Razzo BM, DeSantis ME, Gupta K, Shorter J (2015). The Hsp104 N-terminal domain enables disaggregase plasticity and potentiation. *Mol Cell* 57, 836–849.
- Taxis C, Hitt R, Park SH, Deak PM, Kostova Z, Wolf DH (2003). Use of modular substrates demonstrates mechanistic diversity and reveals differences in chaperone requirement of ERAD. *J Biol Chem* 278, 35903–35913.
- Torrente MP, Chuang E, Noll MM, Jackrel ME, Go MS, Shorter J (2016). Mechanistic insights into Hsp104 potentiation. *J Biol Chem* 291, 5101–5115.
- Vergheze J, Abrams J, Wang Y, Morano KA (2012). Biology of the heat shock response and protein chaperones: budding yeast (*Saccharomyces cerevisiae*) as a model system. *Microbiol Mol Biol Rev* 76, 115–158.
- Wang R, Brattain MG (2007). The maximal size of protein to diffuse through the nuclear pore is larger than 60 kDa. *FEBS Lett* 581, 3164–3170.
- Werner-Washburne M, Becker J, Kosic-Smithers J, Craig EA (1989). Yeast Hsp70 RNA levels vary in response to the physiological status of the cell. *J Bacteriol* 171, 2680–2688.
- Werner-Washburne M, Stone DE, Craig EA (1987). Complex interactions among members of an essential subfamily of hsp70 genes in *Saccharomyces cerevisiae*. *Mol Cell Biol* 7, 2568–2577.